AIAA JOURNAL
Vol. 54, No. 7, July 2016

Technical Notes

TECHNICAL NOTES are short manuscripts describing new developments or important results of a preliminary nature. These Notes should not exceed 2500 words (where a figure or table counts as 200 words). Following informal review by the Editors, they may be published within a few months of the date of receipt. Style requirements are the same as for regular contributions (see inside back cover).

Approximate Projection Method for the Incompressible Navier–Stokes Equations

Francesco Capuano,* Gennaro Coppola,† Matteo Chiatto,‡ and Luigi de Luca§
University of Naples "Federico II", 80125 Naples, Italy

DOI: 10.2514/1.J054569

I. Introduction

IN THE context of time-advancing algorithms for the incompressible Navier–Stokes equations

$$\frac{\partial u_i}{\partial t}+\frac{\partial u_i u_j}{\partial x_j}=-\frac{\partial P}{\partial x_i}+\frac{1}{Re}\frac{\partial^2 u_i}{\partial x_j \partial x_j} \tag{1}$$

$$\frac{\partial u_i}{\partial x_i}=0 \tag{2}$$

the divergence-free condition is commonly enforced by means of so-called projection methods [1]. Typically, the algorithm is articulated into two main stages: at first, a velocity field that does not satisfy the incompressibility constraint is computed; then, a pressure correction is operated to project the intermediate flowfield onto the space of divergence-free velocity fields, with the pressure being obtained by the solution of an ad hoc Poisson equation. Projection methods can hence be interpreted as two-stage fractional step schemes. In principle, projection techniques can be coupled to any time-advancement method, although they are most commonly applied in conjunction with Adams–Bashforth and Crank–Nicolson schemes for the convective and viscous terms, respectively [2,3].

Time integration can also be accomplished by means of multistage Runge–Kutta (RK) methods, which are particularly advantageous thanks to their self-starting capability and relatively large stability regions [4]. Furthermore, the RK coefficients can be optimized for multiple purposes, e.g., achieving a high formal order of temporal accuracy [5], optimizing dissipation and dispersion properties [6], or improving the accuracy of the pressure [7]. Recently, the present authors have developed a RK-based algorithm that mimics the discrete energy-conservation properties of the skew-symmetric form of the nonlinear term at a reduced computational cost by properly weighting spatial and temporal errors [8,9]. Implicit–explicit RK methods can also be constructed to handle stiff problems [10].

The main drawback of Runge–Kutta fractional step methods is that a Poisson equation for pressure has to be solved at each RK substage to impose the incompressibility constraint and retain the temporal order of accuracy of the procedure, leading to a significant increase in computational effort. As a remedy to this issue, Le and Moin [11] proposed to project the velocity field only at the final step; within the intermediate substages, a first-order approximation based on the previous time step was used to compute the pressure gradient. Their modified algorithm, developed for a three-stage semi-implicit Runge–Kutta scheme, led to an overall time savings of about 40%. However, the method was limited to second-order accuracy and, in some cases, might have been susceptible to instabilities due to nonzero divergence of intermediate velocity fields [12].

The aim of this Technical Note is to propose an approximate projection method based on a broader class of Runge–Kutta time-stepping schemes. The pressure correction is operated only at the final step, as in [11]; however, an improved approximation for pressure is used within the substeps to enhance the formal accuracy as well as the robustness of the method.

II. Numerical Method

The numerical procedure is based on the class of standard Runge–Kutta schemes for time integration. The algorithm lies on a classical semidiscrete approach: the Navier–Stokes equations are first discretized in space and then integrated in time. A straightforward s-stage time advancement of a semidiscretized version of Eqs. (1) and (2) reads

$$\begin{cases}\boldsymbol{u}_i=\boldsymbol{u}^n+\Delta t\sum_{j=1}^{s}a_{ij}[\mathcal{L}(\boldsymbol{u}_j)-\mathcal{N}(\boldsymbol{u}_j)-\mathcal{G}(\boldsymbol{p}_j)], & i=1,\ldots,s\\ \boldsymbol{u}^{n+1}=\boldsymbol{u}^n+\Delta t\sum_{i=1}^{s}b_i[\mathcal{L}(\boldsymbol{u}_i)-\mathcal{N}(\boldsymbol{u}_i)-\mathcal{G}(\boldsymbol{p}_j)]\end{cases} \tag{3}$$

where $\boldsymbol{u}\in R^{N_u}$ and $\boldsymbol{p}\in R^{N_p}$ are the discretized velocity and pressure fields; a_{ij} and b_i are the RK coefficients; and $\mathcal{L}$, $\mathcal{N}$, and $\mathcal{G}$ represent proper approximations to the Laplacian, nonlinear, and gradient operators, respectively. In particular, $\mathcal{L}\in R^{N_u\times N_u}$ and $\mathcal{G}\in R^{N_u\times N_p}$ are linear discrete operators, whereas $\mathcal{N}\in R^{N_u}$ is the discretization of the nonlinear convective term and depends upon the formulation adopted for convection (e.g., divergence, advective, skew-symmetric) [9]. It is worth noting that the developments presented in the Note are independent of the spatial discretization technique employed, provided that the operators are discretized consistently, i.e., $\mathcal{G}^T=-\mathcal{D}$, where $\mathcal{D}\in R^{N_p\times N_u}$ is the discrete divergence operator and $(\cdot)^T$ denotes transposition. In Eq. (3) and hereinafter, subscripts refer to the RK substep, whereas superscripts denote the time level. Starred velocity fields are not divergence free.

In a classical fractional-step method, the pressure constraint in Eq. (3) is most conveniently enforced by means of the usual splitting:

$$\begin{cases}\boldsymbol{u}_i^*=\boldsymbol{u}^n+\Delta t\sum_{j=1}^{s}a_{ij}[\mathcal{L}(\boldsymbol{u}_j)-\mathcal{N}(\boldsymbol{u}_j)],\\ \mathcal{D}\mathcal{G}(\phi_i)=\frac{1}{c_i\Delta t}\mathcal{D}(\boldsymbol{u}_i^*),\\ \boldsymbol{u}_i=\boldsymbol{u}_i^*-c_i\Delta t\mathcal{G}(\phi_i), \qquad i=2,\ldots,s\end{cases} \tag{4}$$

where ϕ_i is a pseudopressure that acts as a Lagrange multiplier to ensure the divergence-free condition for each $\boldsymbol{u}_i^*$, and $c_i=\sum_j a_{ij}$. In

Received 23 June 2015; revision received 14 January 2016; accepted for publication 7 February 2016; published online 24 May 2016.

*Researcher, Dipartimento di Ingegneria Industriale.
†Associate Professor, Dipartimento di Ingegneria Industriale.
‡Ph.D. Student, Dipartimento di Ingegneria Industriale.
§Full Professor, Dipartimento di Ingegneria Industriale.

general, the Lagrange multiplier is a first-order approximation to the pressure [13]:

$$\phi_i = \boldsymbol{p}_i + \mathcal{O}(\Delta t) \tag{5}$$

The algorithm that results from combining Eq. (4) with Eq. (3) will be referred to as FS, to indicate a traditional RK-based fractional-step scheme. In the case of explicit methods, s Poisson equations have to be solved for pressure: $(s-1)$ for the intermediate stages (assuming $\boldsymbol{u}^n$ is divergence free), and a final one after the last step to project $\boldsymbol{u}^{n+1,*}$.

A significant savings in CPU time can be obtained if one seeks to solve only one Poisson equation after the last step. This task can be accomplished by using a suitable approximation for the pseudopressure within the midstages based on the previous time steps, e.g.,

$$\phi_i \approx \hat{\phi}_i = F(\phi^n, \phi^{n-1}) \tag{6}$$

In particular, two methods will be considered here:

$$\hat{\phi}_i = \phi^n$$

and

$$\hat{\phi}_i = \frac{3\phi^n - \phi^{n-1}}{2} + (\phi^n - \phi^{n-1})\frac{c_i}{2}$$

which correspond to constant and linear extrapolations from previous values, respectively. The second approximation has been derived by constructing a linear interpolant for the pressure $\boldsymbol{p}$ (that is, the physically relevant variable) from $t^{n-3/2}$ to $t^{n-1/2}$ and by evaluating the formula at $t^{n+c_i/2}$. This choice comes from the fact that consistent second-order estimates of $\boldsymbol{p}^{n-3/2}$, $\boldsymbol{p}^{n-1/2}$, and $\boldsymbol{p}^{n+c_i/2}$ are available from ϕ^{n-1}, ϕ^n, and ϕ_i, respectively, by virtue of the midpoint method [7].

The resulting algorithm can be written as follows:

$$\begin{cases} \hat{\boldsymbol{u}}_i = \boldsymbol{u}^n + \Delta t \sum_{j=1}^{s} a_{ij}[\mathcal{L}(\hat{\boldsymbol{u}}_j) - \mathcal{N}(\hat{\boldsymbol{u}}_j)] - c_i \Delta t \mathcal{G}(\hat{\phi}_i), \quad i = 1, \ldots, s, \\ \boldsymbol{u}^{n+1,*} = \boldsymbol{u}^n + \Delta t \sum_{i=1}^{s} b_i[\mathcal{L}(\hat{\boldsymbol{u}}_i) - \mathcal{N}(\hat{\boldsymbol{u}}_i)], \\ \mathcal{D}\mathcal{G}(\phi^{n+1}) = \frac{1}{\Delta t}\mathcal{D}(\boldsymbol{u}^{n+1,*}), \\ \boldsymbol{u}^{n+1} = \boldsymbol{u}^{n+1,*} - \Delta t \mathcal{G}(\phi^{n+1}) \end{cases} \tag{7}$$

No Poisson equations have to be solved for stages $i = 1, \ldots, s$, but a final projection step is still required for $\boldsymbol{u}^{n+1,*}$. Depending on the choice made for $\hat{\phi}_i$, the algorithms will be labeled FSa and FSb for constant and linear extrapolation, respectively. Note that the method labeled FSa is actually a generalization of the procedure proposed in [11], and it turns out to be second-order accurate, assuming the time-integration scheme is at least second order. It can be shown that the new method labeled FSb is third-order accurate in time on velocity; the accuracy of both methods will be demonstrated numerically in the next section.

It is interesting to mention that a similar higher-order extrapolation for pressure has proved to also be beneficial for an approximate pressure-correction method developed in the context of two-phase incompressible flows [14].

III. Results

A. Order of Accuracy Study

The two-dimensional Taylor–Green vortex is simulated numerically to confirm the theoretical results presented in the previous sections. The Navier–Stokes equations are solved in a periodic domain of length 2π, and they are discretized on a uniform mesh of 20^2 points. The exact solution is given by

$$\begin{aligned} u_e(x, y, t) &= -\cos(x)\,\sin(y)e^{-2t/Re}, \\ v_e(x, y, t) &= \sin(x)\,\cos(y)e^{-2t/Re}, \\ p_e(x, y, t) &= -\frac{1}{4}(\cos(2x) + \cos(2y))e^{-4t/Re} \end{aligned} \tag{8}$$

Starting from $t = 0$, Eq. (8) is solved numerically with a standard pseudospectral method [15]. The skew-symmetric form $(\text{Skew.})_i$ of the nonlinear convective term, given by

$$(\text{Skew.})_i = \frac{1}{2}\frac{\partial u_j u_i}{\partial x_j} + \frac{1}{2}u_j\frac{\partial u_i}{\partial x_j} \tag{9}$$

is discretized, which guarantees semidiscrete conservation of kinetic energy in the inviscid limit. This property is of fundamental importance to enforce a nonlinear stability bound to the numerical solution [16]. The standard three-stage third-order-explicit Kutta rule is used for time integration [4], in conjunction with the three algorithms presented in Sec. II. The temporal order of accuracy is shown in Fig. 1 for $Re = 100$. The time-step convergence of the L2 norm of the velocity error is calculated at $t_f = -Re\,\log(\sqrt{0.9})$, at which the vortices' intensity has reduced to the 90% of the initial value. The results confirm that the method FSb is third-order accurate, while FSa is second order. The methods labeled FSb and FS are both third-order accurate, although the magnitude of the error provided by the former is larger due to the approximation for pressure used within the substeps.

In Fig. 2, the L_∞ norm of the residual divergence of the velocity fields $\hat{\boldsymbol{u}}_i$ at the RK substeps is compared for the various methods at $t = t_f$, $\Delta t = 0.1$, and $Re = 100$. The velocity field $\boldsymbol{u}_1$ does not need to be projected, assuming that $\boldsymbol{u}^n$ is divergence free. For the substeps $i = 2$ and $i = 3$, the method labeled FSb provides lower divergence

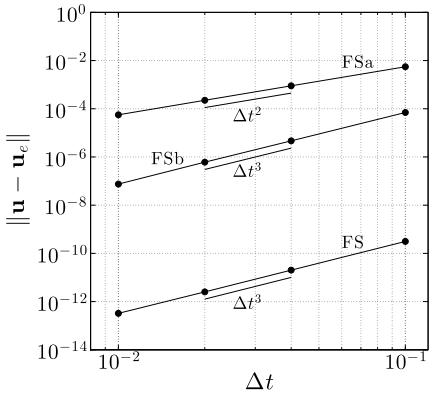

Fig. 1 Time-step convergence of velocity error for the three projection methods: FS, FSa, and FSb. Filled circles represent the data, and $Re = 100$.

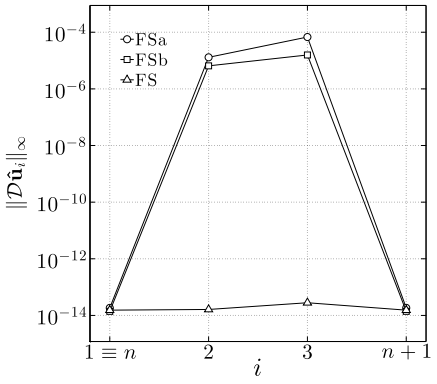

Fig. 2 L_∞ norm of the residual divergence of velocity at each RK substep, calculated at $t = t_f$ for the three methods: $\Delta t = 0.1$, and $Re = 100$.

errors with respect to the FSa. It is worth remarking that, at the full time step, the maximum value of the velocity divergence over the domain is zero to machine precision for both methods labeled FSa and FSb, whereas the FS method provides divergence-free velocity fields at each RK substep.

The accuracy of the pseudopressure ϕ has also been calculated; in all cases, it is a first-order approximation of the pressure p_e, in accordance with Eq. (6). This result can be improved by either satisfying additional conditions for the Runge–Kutta coefficients or by solving an additional Poisson equation at t^{n+1} [7].

B. Three-Dimensional Taylor–Green Vortex

A more challenging test is the three-dimensional Taylor–Green vortex at high Reynolds numbers. In this case, the initial distribution of vorticity is subject to vortex stretching, thus generating smaller scales and eventually leading to turbulence breakdown [15]. A triperiodic cube is filled by the initial conditions

$$\begin{aligned} u(x,y,z,0) &= \frac{2}{\sqrt{3}}\,\sin\left(\theta+\frac{2}{3}\pi\right)\,\sin(x)\,\cos(y)\,\cos(z)\\ v(x,y,z,0) &= \frac{2}{\sqrt{3}}\,\sin\left(\theta-\frac{2}{3}\pi\right)\cos(x)\,\sin(y)\,\cos(z)\\ w(x,y,z,0) &= \frac{2}{\sqrt{3}}\,\sin(\theta)\,\cos(x)\,\cos(y)\,\sin(z) \end{aligned} \tag{10}$$

with $\theta = 0$. Equation (10) is time advanced by the same numerical method used for the previous test. The Reynolds number of $Re = 1600$ is chosen to be sufficiently high in order to trigger transition to turbulence, which occurs around $t = 9$. An under-resolved uniform computational mesh of 32^3 points is used, and no subgrid-scale models are employed. Although this setting is not physically relevant, it is useful to test the robustness of the solution algorithm.

The various methods are evaluated by means of the time evolution of the derivative skewness

$$Sk_{11} = -\int_\Omega \left(\frac{\partial u}{\partial x}\right)^3 \Big/ \left(\int_\Omega \left(\frac{\partial u}{\partial x}\right)^2\right)^{3/2} \tag{11}$$

integrated over the computational domain Ω. The skewness is a fundamental quantity in turbulent flows, as it represents the rate of production of vorticity through vortex stretching [17]. The results are shown in Fig. 3. Despite the under-resolution, all the computations are stable due to the use of a spatially energy-conserving method. However, the three methods are in close agreement only until $t \approx 9$. Subsequently, the flow breaks into turbulence and the FSa method starts to significantly deviate from the other two. In contrast, the FS and FSb results display the same evolution at later times.

Other integral quantities (such as kinetic energy dissipation rate, derivative flatness, enstrophy, etc., which are not shown here) follow a similar pattern.

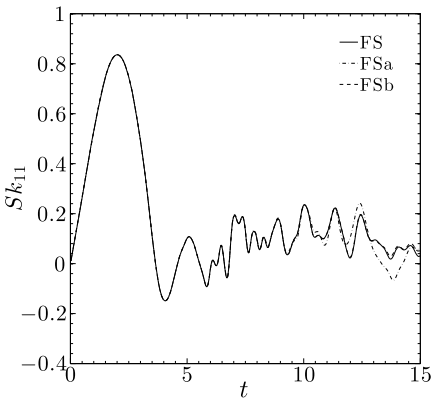

Fig. 3 Time evolution of integral derivative skewness for the three projection methods: FS, FSa, and FSb.

C. Performances

The performances of the method are highly dependent upon the specific features of the overall solution procedure, the models adopted, the implementation details, as well as the computational architecture. The test presented in Sec. III.A was also performed using a colocated energy-conserving second-order finite difference code [18], with the pressure Poisson equation solved in physical space by the biconjugate gradient stabilized method [19]. In this case, the approximate fractional-step methods provide computational time savings of about 50% with respect to the FS. A further reduction of the CPU time can be obtained by adopting the alternating Runge–Kutta procedure developed in [8,9] to halve the cost of the skew-symmetric splitting: in this case, an extra 10% savings was achieved with respect to the FS method in fully skew-symmetric form.

IV. Conclusions

An approximate projection method has been developed for the incompressible Navier–Stokes equations. The algorithm was based on a generic family of Runge–Kutta time-stepping schemes, and it was particularly efficient from a computational point of view since the pressure projection step was operated only at the final stage. In contrast to previously developed methods, the new procedure employed a higher-order approximation for pressure within the substages, and hence allowed achievement of third-order temporal accuracy for the velocity field. Also, by improving the pressure approximation, the divergence error at each substep could be significantly reduced, leading to enhanced robustness. Preliminary turbulent simulations demonstrated the effectiveness of the method. The formulation was general and could, in principle, accommodate Runge–Kutta methods of any class and type.

Acknowledgment

The first two authors would like to acknowledge Parviz Moin for promoting discussions on this and related topics during the Summer Program 2014 of the Center for Turbulence Research at Stanford University.

References

[1] Chorin, A., "Numerical Solution of the Navier–Stokes Equations," *Mathematics of Computation*, Vol. 22, No. 104, 1968, pp. 745–745. doi:10.1090/S0025-5718-1968-0242392-2

[2] Kim, J., and Moin, P., "Application of a Fractional-Step Method to Incompressible Navier–Stokes Equations," *Journal of Computational Physics*, Vol. 59, No. 2, 1985, pp. 308–323. doi:10.1016/0021-9991(85)90148-2

[3] Bell, J. B., Solomon, J. M., and Szymczak, W. G., "Projection Method for Viscous Incompressible Flow on Quadrilateral Grids," *AIAA Journal*, Vol. 32, No. 10, 1994, pp. 1961–1969. doi:10.2514/3.12239

[4] Griffiths, D. F., and Higham, D. J., *Numerical Methods for Ordinary Differential Equations*, Springer, New York, 2010, pp. 123–140.

[5] Butcher, J., *Numerical Methods for Ordinary Differential Equations*, Wiley, Hoboken, NJ, 2004, pp. 93–104.

[6] Hu, F. Q., Hussaini, M. Y., and Manthey, J. L., "Low-Dissipation and Low-Dispersion Runge–Kutta Schemes for Computational Acoustics," *Journal of Computational Physics*, Vol. 124, No. 1, 1996, pp. 177–191. doi:10.1006/jcph.1996.0052

[7] Sanderse, B., and Koren, B., "Accuracy Analysis of Explicit Runge–Kutta Methods Applied to the Incompressible Navier–Stokes Equations," *Journal of Computational Physics*, Vol. 231, No. 8, 2012, pp. 3041–3063. doi:10.1016/j.jcp.2011.11.028

[8] Capuano, F., Coppola, G., and de Luca, L., "An Efficient Time Advancing Strategy for Energy-Preserving Simulations," *Journal of Computational Physics*, Vol. 295, Aug. 2015, pp. 209–229. doi:10.1016/j.jcp.2015.03.070

[9] Capuano, F., Coppola, G., and de Luca, L., "Energy Preserving Turbulent Simulations at a Reduced Computational Cost," *Journal of Computational Physics*, Vol. 298, Oct. 2015, pp. 480–494. doi:10.1016/j.jcp.2015.06.011

[10] Yoh, J. J., and Zhong, X., "New Hybrid Runge–Kutta Methods for Unsteady Reactive Flow Simulation," *AIAA Journal*, Vol. 42, No. 8,

2004, pp. 1593–1600.
doi:10.2514/1.3843

[11] Le, H., and Moin, P., "An Improvement of Fractional Step Methods for the Incompressible Navier–Stokes Equations," *Journal of Computational Physics*, Vol. 92, No. 2, 1991, pp. 369–379.
doi:10.1016/0021-9991(91)90215-7

[12] Sullivan, P. P., McWilliams, J. C., and Patton, E. G., "Large-Eddy Simulation of Marine Atmospheric Boundary Layers above a Spectrum of Moving Waves," *Journal of the Atmospheric Sciences*, Vol. 71, Nov. 2014, pp. 4001–4027.
doi:10.1137/0913035

[13] Perot, J., "Comments on the Fractional Step Method," *Journal of Computational Physics*, Vol. 121, No. 1, 1995, pp. 190–191.
doi:10.1006/jcph.1995.1189

[14] Dodd, M. S., and Ferrante, A., "A Fast Pressure-Correction Method for Incompressible Two-Fluid Flows," *Journal of Computational Physics*, Vol. 273, Sept. 2014, pp. 416–434.
doi:10.1016/j.jcp.2014.05.024

[15] Canuto, C., Hussaini, M.Y., Quarteroni, A., and Zang, T. A., *Spectral Methods. Evolution to Complex Geometries and Applications to Fluid Dynamics*, Springer, New York, 2007, PP. 98–99.

[16] Verstappen, R. W. C. P., and Veldman, A. E. P., "Symmetry-Preserving Discretization of Turbulent Flow," *Journal of Computational Physics*, Vol. 187, No. 1, 2003, pp. 343–368.
doi:10.1016/S0021-9991(03)00126-8

[17] Monin, A. S., and Yaglom, A. M., *Statistical Fluid Mechanics: Mechanics of Turbulence*, Vol. 2, MIT Press, Cambridge, MA, 1975, p. 58.

[18] Shashank, L. J., and Iaccarino, G., "A Co-Located Incompressible Navier–Stokes Solver with Exact Mass, Momentum and Kinetic Energy Conservation in the Inviscid Limit," *Journal of Computational Physics*, Vol. 229, No. 12, 2010, pp. 4425–4430.
doi:10.1016/j.jcp.2010.03.010

[19] van der Vorst, H. A., "BI-CGSTAB: A Fast and Smoothly Converging Variant of BI-CG for the Solution of Nonsymmetric Linear Systems," *SIAM Journal on Scientific and Statistical Computing*, Vol. 13, No. 2, 1992, pp. 631–644.
doi:10.1137/0913035

G. Blaisdell
Associate Editor